Crustal structure of the Mid Black Sea High from wide-angle seismic data

D. J. SHILLINGTON[1]*, T. A. MINSHULL[2], R. A. EDWARDS[3] & N. WHITE[4]

[1]*Lamont-Doherty Earth Observatory of Columbia University, 61 Route 9W, Palisades, NY 10964, USA*

[2]*Ocean and Earth Science, National Oceanography Centre Southampton, University of Southampton, European Way, Southampton SO14 3ZH, UK*

[3]*National Oceanography Centre, European Way, Southampton SO14 3ZH, UK*

[4]*Bullard Laboratories, University of Cambridge, Madingley Rise, Madingley Road, Cambridge CB3 0EZ, UK*

**Correspondence: djs@ldeo.columbia.edu*

Abstract: The Mid Black Sea High comprises two en echelon basement ridges, the Archangelsky and Andrusov ridges, that separate the western and eastern Black Sea basins. The sediment cover above these ridges has been characterized by extensive seismic reflection data, but the crustal structure beneath is poorly known. We present results from a densely sampled wide-angle seismic profile, coincident with a pre-existing seismic reflection profile, which elucidates the crustal structure. We show that the basement ridges are covered by approximately 1–2 km of pre-rift sedimentary rocks. The Archangelsky Ridge has higher pre-rift sedimentary velocities and higher velocities at the top of basement (*c.* 6 km s^{-1}). The Andrusov Ridge has lower pre-rift sedimentary velocities and velocities less than 5 km s^{-1} at the top of the basement. Both ridges are underlain by approximately 20-km-thick crust with velocities reaching around 7.2 km s^{-1} at their base, interpreted as thinned continental crust. These high velocities are consistent with the geology of the Pontides, which is formed of accreted island arcs, oceanic plateaux and accretionary complexes. The crustal thickness implies crustal thinning factors of approximately 1.5–2. The differences between the ridges reflect different sedimentary and tectonic histories.

Several episodes of extension and shortening have shaped the Black Sea region since Permian times (e.g. Yilmaz *et al.* 1997; Nikishin *et al.* 2003; Robertson *et al.* 2004), which led to the addition of a series of volcanic arcs, oceanic plateaux and accretionary complexes to the Eurasian margin (e.g. Okay *et al.* 2013). The basin is thought to have formed in a back-arc extensional environment because of its close spatial association with the subduction of both the Palaeo- and Neo-Tethys oceans (e.g. Letouzey *et al.* 1977), but the timing and style of this opening history remain controversial, partly because the thick sediment cover means that the oldest sedimentary fill has not been drilled (Zonenshain & Le Pichon 1986; Okay *et al.* 1994, 2017; Banks *et al.* 1997; Nikishin *et al.* 2015*a*). The Black Sea is commonly subdivided into eastern and western basins; these sub-basins are separated by the Mid Black Sea High (MBSH), a system of buried basement ridges that runs SW–NE (Fig. 1) (e.g. Okay *et al.* 1994; Nikishin *et al.* 2015*a*).

The opening of the western basin may be estimated from the ages of arc volcanic rocks in the Western Pontides and from associated plate reconstructions; this evidence suggests a Middle–Upper Cretaceous age (Görür 1988; Okay *et al.* 1994, 2017). Based on seismic refraction and gravity data, the crust in the centre of the basin is 7–8 km thick and has velocities consistent with the presence of oceanic crust, suggesting that rifting culminated in seafloor spreading (Letouzey *et al.* 1977; Belousov *et al.* 1988; Starostenko *et al.* 2004).

The age and nature of the eastern basin are more controversial. The basin is thought to have formed by rotation of the Shatsky Ridge relative to the MBSH (Figs 1 & 2) (Okay *et al.* 1994; Nikishin *et al.* 2003). The main phase of opening has been interpreted as Jurassic, Cretaceous (Zonenshain & Le Pichon 1986; Okay *et al.* 1994; Nikishin *et al.* 2003, 2015*b*), Early Eocene–Paleocene (Robinson *et al.* 1995; Banks *et al.* 1997; Shillington *et al.* 2008) or Eocene (Kazmin *et al.* 2000; Vincent *et al.* 2005). Based on gravity and early seismic data, the crust in the centre of this basin was inferred to have a thickness of approximately 10–11 km and

From: Simmons, M. D., Tari, G. C. & Okay, A. I. (eds) *Petroleum Geology of the Black Sea*. Geological Society, London, Special Publications, **464**, https://doi.org/10.1144/SP464.6

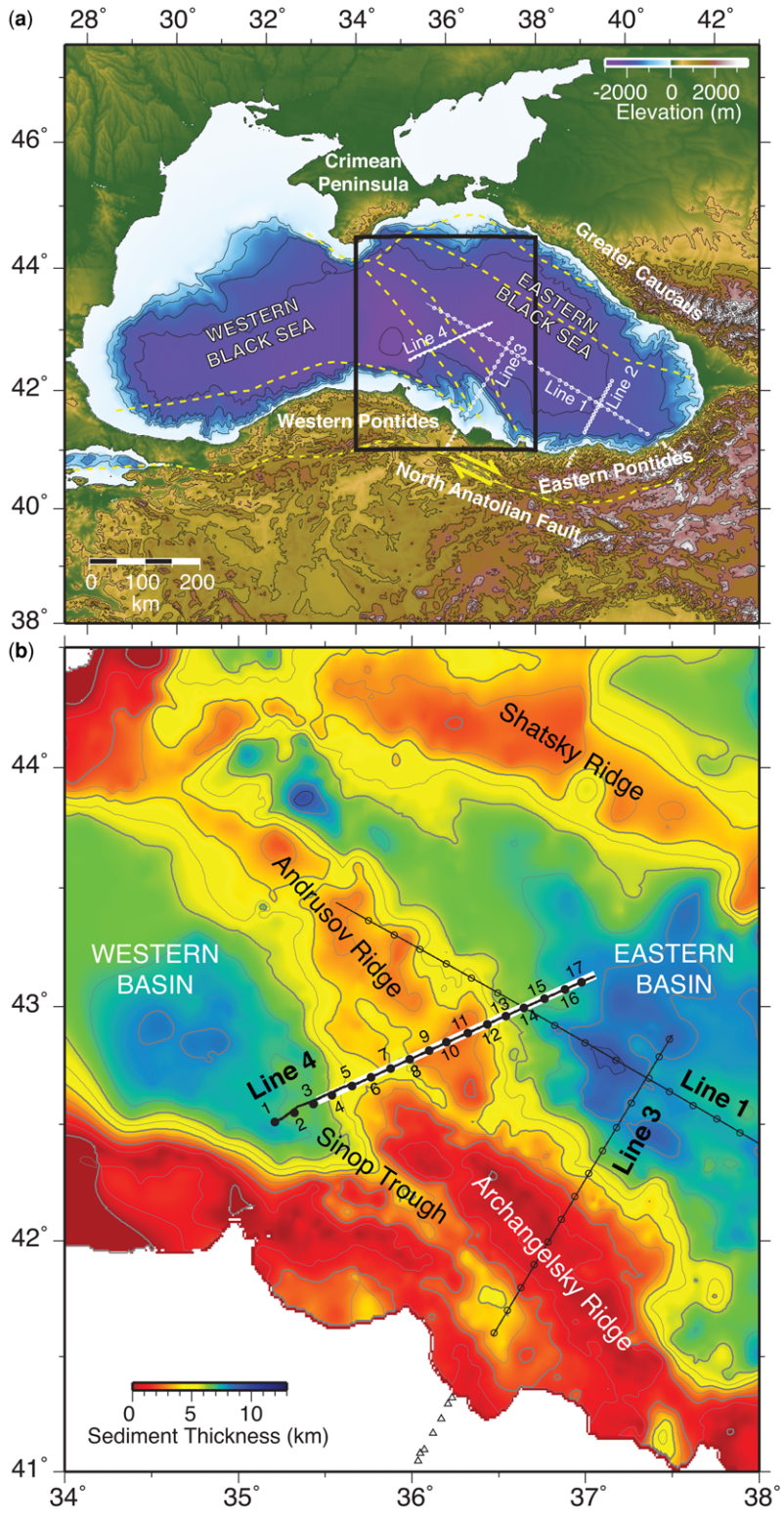
(a)
28°
30°
32°
34°
36°
38°
40°
42°
46°
44°
42°
40°
38°
-2000 0 2000
Elevation (m)
Crimean Peninsula
Greater Caucasus
WESTERN BLACK SEA
EASTERN BLACK SEA
Line 4
Line 3
Line 1
Line 2
Western Pontides
Eastern Pontides
North Anatolian Fault
0 100 200
km
(b)
44°
43°
42°
41°
34°
35°
36°
37°
38°
Shatsky Ridge
Andrusov Ridge
WESTERN BASIN
EASTERN BASIN
Line 4
Line 1
Line 3
Sinop Trough
Archangelsky Ridge
0 5 10
Sediment Thickness (km)

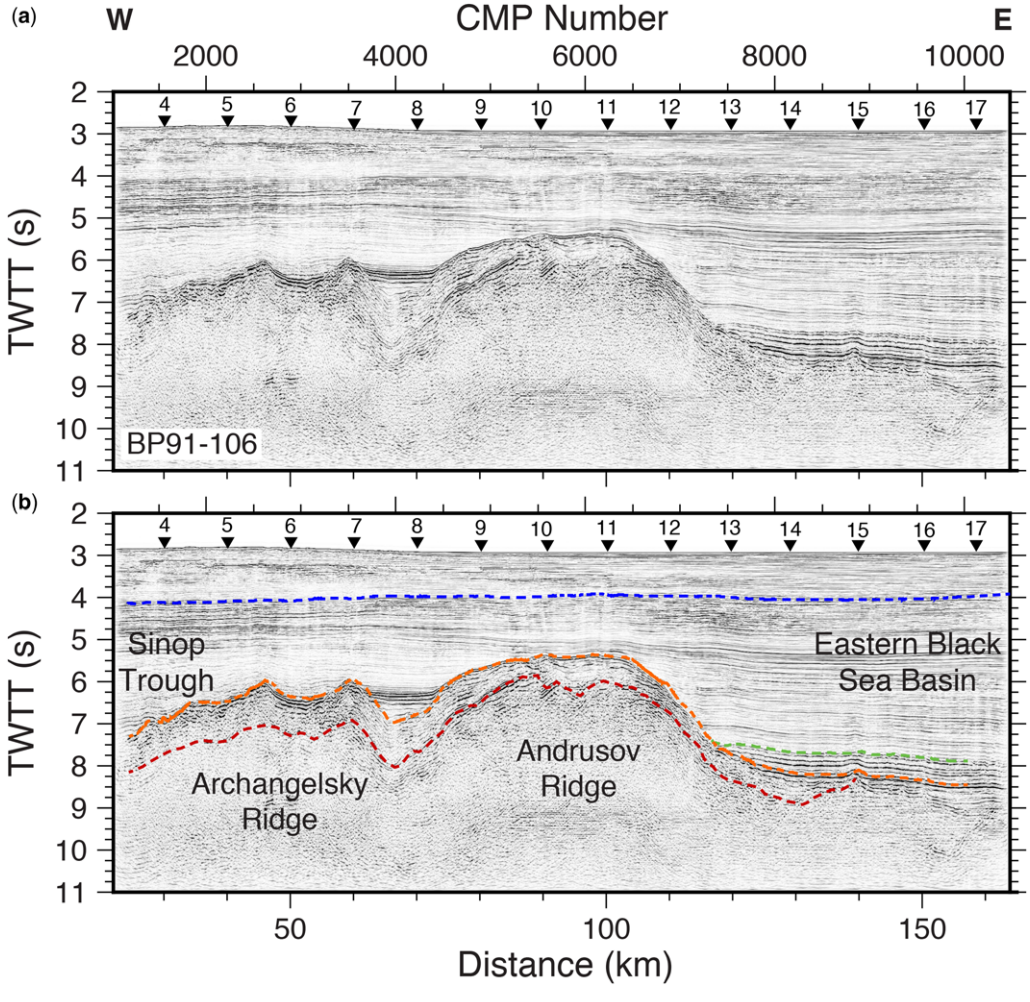

Fig. 2. (**a**) Seismic reflection profile 91–106 across the Mid-Black Sea High, which is coincident with the Line 4 OBS profile (courtesy of BP and TPAO) (see Fig. 1 for the location). (**b**) Seismic reflection profile with interfaces used in seismic inversion. The blue, green and orange dotted lines show interpreted horizons used to invert for post- and syn-rift sedimentary structure by Scott *et al.* (2009). The red dotted line shows the interpreted pre-rift sedimentary horizon used in the inversions presented here.

lower seismic velocities than those of typical oceanic crust, suggesting the presence of thinned continental crust (Belousov *et al.* 1988; Starostenko *et al.* 2004). However, results from a wide-angle seismic experiment in 2005 suggest that the crustal structure varies along the basin, with the western

Fig. 1. (**a**) Elevation/bathymetry of the Black Sea region from GEBCO showing the location of the 2005 onshore/offshore seismic refraction experiment. Shot lines are indicated with white lines, OBS are shown with white circles and seismometers deployed onshore are shown with white triangles. OBS from Line 4, which are used in this study, are indicated with solid circles. Major tectonic elements indicated with dashed yellow lines (Zonenshain & Le Pichon 1986). The black box indicates the area shown in (b). (**b**) Close-up of the Mid Black Sea High showing sediment thickness (Shillington *et al.* 2008) and OBS locations and shot lines from the 2005 experiment in black. Note that the Mid Black Sea High separates the western and eastern basins of the Black Sea and comprises two ridges: the Archangelsky Ridge and the Andrusov Ridge. Seismic reflection profile 91–106 (Fig. 2) is shown with thick white line. It is coincident with Profile 4 but shorter; it extends SW to between OBS 3 and 4.

part floored by thinned continental crust (7–9 km thick), and thicker, higher velocity crust below the eastern part that is attributed to magmatically robust early seafloor spreading resulting in early oceanic crust that is thicker and has higher velocities than average oceanic crust (Shillington *et al.* 2009).

The MBSH itself is divided into the en echelon Archangelsky and Andrusov ridges, which have different sediment thicknesses and are inferred to have different structure and origin (Robinson *et al.* 1996; Nikishin *et al.* 2015*a*) (Fig. 1b). These ridges are poorly explored compared to the basins on either side. The Andrusov Ridge is inferred to have formed during early opening of the eastern basin (Okay *et al.* 1994; Robinson *et al.* 1996; Nikishin *et al.* 2015*b*). This rifting event is inferred to have been amagmatic in this part of the basin (Shillington *et al.* 2009). Alternatively, the Andrusov Ridge is interpreted as a marginal ridge associated with the opening of the western basin along the West Crimean Transform Fault (Tari *et al.* 2015). The Archangelsky Ridge was formed by the opening of the Sinop Trough, which is linked to the western basin and is interpreted to have opened in Cretaceous–Paleocene times (Robinson *et al.* 1996; Espurt *et al.* 2014), with ongoing extension into the Miocene (Rangin *et al.* 2002; Espurt *et al.* 2014). An Upper Cretaceous sedimentary sequence and lower Cretaceous platform carbonate rocks have been dredged where the pre-rift sequences crop out on the flank of Archangelsky Ridge, providing an upper limit on its age of formation (Rudat *et al.* 1993; Robinson *et al.* 1996).

After their formation, both ridges have also experienced compressional deformation (Rangin *et al.* 2002; Espurt *et al.* 2014). This region has probably experienced multiple episodes of compression, continuing to the present; apatite fission-track data and palaeostress measurements onshore show that inversion of rifting structure onshore occurred as early as 55 Ma (Saintot & Angelier 2002; Espurt *et al.* 2014), following extension leading to the opening of eastern Black Sea. Active compression continues around margins of the easternmost Black Sea today based on seismicity and onshore geology, particularly in the Caucaus (Saintot & Angelier 2002; Gobarenko *et al.* 2016).

Published constraints on crustal structure beneath the ridges are sparse. Seismic refraction data acquired in the 1960s were recently re-analysed using modern ray-tracing techniques (Yegorova & Gobarenko 2010). This analysis suggests a crustal thickness of approximately 20 km beneath both ridges and crustal velocities in the range 6.0–7.0 km s^{-1}, interpreted as representing thinned continental crust. A profile crossing the southern part of Archangelsky Ridge acquired in 2005 suggests that here, crustal thickness reaches about 25 km (Shillington *et al.* 2009). In this paper we present results from a modern, densely sampled wide-angle seismic profile acquired in 2005 that crosses the Andrusov Ridge close to its southern tip and the Archangelsky Ridge at its northern tip (Fig. 1).

Wide-angle seismic data

An onshore-offshore wide-angle seismic dataset was collected in 2005 using the R/V *Iskatel* to determine the deep structure of the eastern basin and Mid Black Sea High (Minshull *et al.* 2005). Seventeen four-component short-period ocean-bottom seismometers (OBS) from GeoPro GmbH were deployed on Profile 4 across the Andrusov Ridge (Fig. 1; Table 1), and they recorded seismic shots generated from an airgun array with a total volume of 3140 in^3 that was triggered every 90 s (shot spacing *c.* 150 m). Profile 4 was co-located with existing industry seismic reflection data: reflection profile 91–106 (Figs 1 & 2).

Data analysis

Data processing

Water-wave arrivals were used to relocate OBS positions on the seafloor, using a seafloor depth determined by echosounder at the position of each deployment and a water velocity of 1.47 km s^{-1}. Relocated positions were typically less than 75 m from deployment positions, but three OBS have relocated positions that differ by 200–300 m from deployment positions. We applied a minimum phase band-phase filter with corners at 3, 5, 15 and 20 Hz to suppress noise, and applied offset-dependent gains and a reduction velocity of 8 km s^{-1}.

Table 1. *Relocated OBS positions*

OBS	Latitude (°N)	Longitude (°E)
1	42.511005	35.212699
2	42.549179	35.322692
3	42.589855	35.432331
4	42.625923	35.543609
5	42.663829	35.654865
6	42.701	35.766201
7	42.738536	35.876911
8	42.777019	35.987457
9	42.813636	36.09951
10	42.851139	36.21101
11	42.887451	36.323356
12	42.925537	36.434604
13	42.960388	36.540924
14	42.995098	36.645301
15	43.035087	36.765087
16	43.073787	36.882984
17	43.10337	36.974617

Phase identification

We identified refractions and wide-angle reflections from the pre-rift sedimentary section, the crust and the upper mantle that could be consistently identified on a majority of the receiver gathers. Phase interpretations and velocity models of the overlying syn- and post-rift sedimentary section have been presented elsewhere (Scott *et al.* 2009). Travel-time picks were made manually of the following phases: reflections off the base of an interpreted pre-rift sedimentary layer (PprP); crustal refractions (Pg); reflections from the base of the crust (PmP); and upper-mantle refractions (Pn) (Fig. 3; Table 2). Reflections from the base of the interpreted pre-rift sedimentary section are observed from near-vertical incidence to offsets up to approximately 30 km and have picking uncertainties of 30–50 ms. Crustal refractions are observed as first arrivals at offsets from approximately 12 to 100 km and have picking uncertainties of 30–75 ms. Reflections from the base of the crust are observed at offsets between approximately 35 and 100 km; the offsets where PmP reflections are observed vary significantly over the line, indicating variations in crustal thickness. Likewise, the amplitude and character of PmP reflections is also highly variable and thus picks of this phase have relatively high uncertainties of 125 ms. We observed limited and relatively low-amplitude refractions interpreted to arise from the upper mantle in some receiver gathers; these refractions are weak and variable, and have a picking uncertainty of 125 ms. Figure 3 shows examples of OBS data, phase identifications and associated ray paths.

Wide-angle reflections interpreted to originate from the base of the interpreted pre-rift sedimentary layer can be linked to a coincident industry seismic reflection profile (BP91–106, Fig. 2). Picks of this interface were thus also made on the reflection profile (Fig. 2, red dotted line) and included in the inversion. We assigned an uncertainty of 100 ms to these picks to account for uncertainties in associating multichannel seismic reflection (MCS) and wide-angle reflections, and for small-scale variations in interface geometry that cannot be recovered by inversion.

Velocity modelling

The travel-time picks described above were used to invert for velocities of the pre-rift sedimentary section, crust and upper mantle. We used JIVE3D, a regularized tomographic inversion code (Hobro *et al.* 2003), which solves for a minimum structure layer-interface model that fits the data within its uncertainties. Velocities within each layer and interface depths are defined by splines and vary smoothly; interfaces represent velocity discontinuities. The forward problem involves tracing a fan of rays from each OBS position through specified layers in the model to generate predicted travel times (i.e. ray shooting); the ray that arrives within a distance tolerance of the target with the minimum travel time is used. Inversion involves a sequence of linear steps to reduce the difference between observed and predicted travel times (e.g. Figs 4d & 5d), and satisfy other smoothing criteria. In each step, smoothing is reduced and structure is allowed to develop to improve data fit. Smoothing is implemented during inversion by minimizing a function of data misfit and model roughness.

We employed a layer-stripping approach for this line. The previously determined velocity structure of the post- and syn-rift sediment from Scott *et al.* (2009) was held fixed. We first inverted for the interpreted pre-rift sediment layer using picks of wide-angle reflections from OBS data and vertically incident reflections from the coincident seismic reflection profile (Fig. 2). This layer was then held fixed during the inversion for crustal and upper-mantle structure. The inversion converged more quickly and stably for both the pre-rift sedimentary section and for the crustal–mantle sections when we inverted for them separately. However, inverting for all layers simultaneously yielded the same overall velocity structure. We also performed two different inversions for crust–mantle structure. The first inversion used only first-arriving refractions from the crust and mantle. The second inversion included interpreted wide-angle reflections from the base of the crust (PmP) in addition to the first arrivals. The purpose of performing two inversions for the crust and upper mantle structure was to assess which features in the model arise from the inclusion of wide-angle reflections from the base of the crust; identifying PmP is associated with more uncertainty and subjectivity than first arrivals. We are most confident of features that are present in both the first-arrival and reflection/refraction tomographic inversions, and more cautious of features that are primarily constrained by the PmP reflections.

We used a grid spacing of 1×0.5 km in the pre-rift interval, and 1×1 km in the crust and upper mantle. For both inversions, we applied twice as much horizontal smoothing than vertical smoothing and allowed more interface roughness than velocity roughness. A simple 1D velocity model and constant interfaces were used for the starting models in both inversions.

The inversion for the pre-rift layer used 825 picks from the OBS data and 129 picks from the MCS data. The final model has a chi-squared misfit of 1.29 and RMS residual of 72 ms if only the OBS picks are included. Larger misfits are associated with the MCS picks since they include smaller-scale variations in interface geometry than can be recovered by the inversion. If these are included, the overall

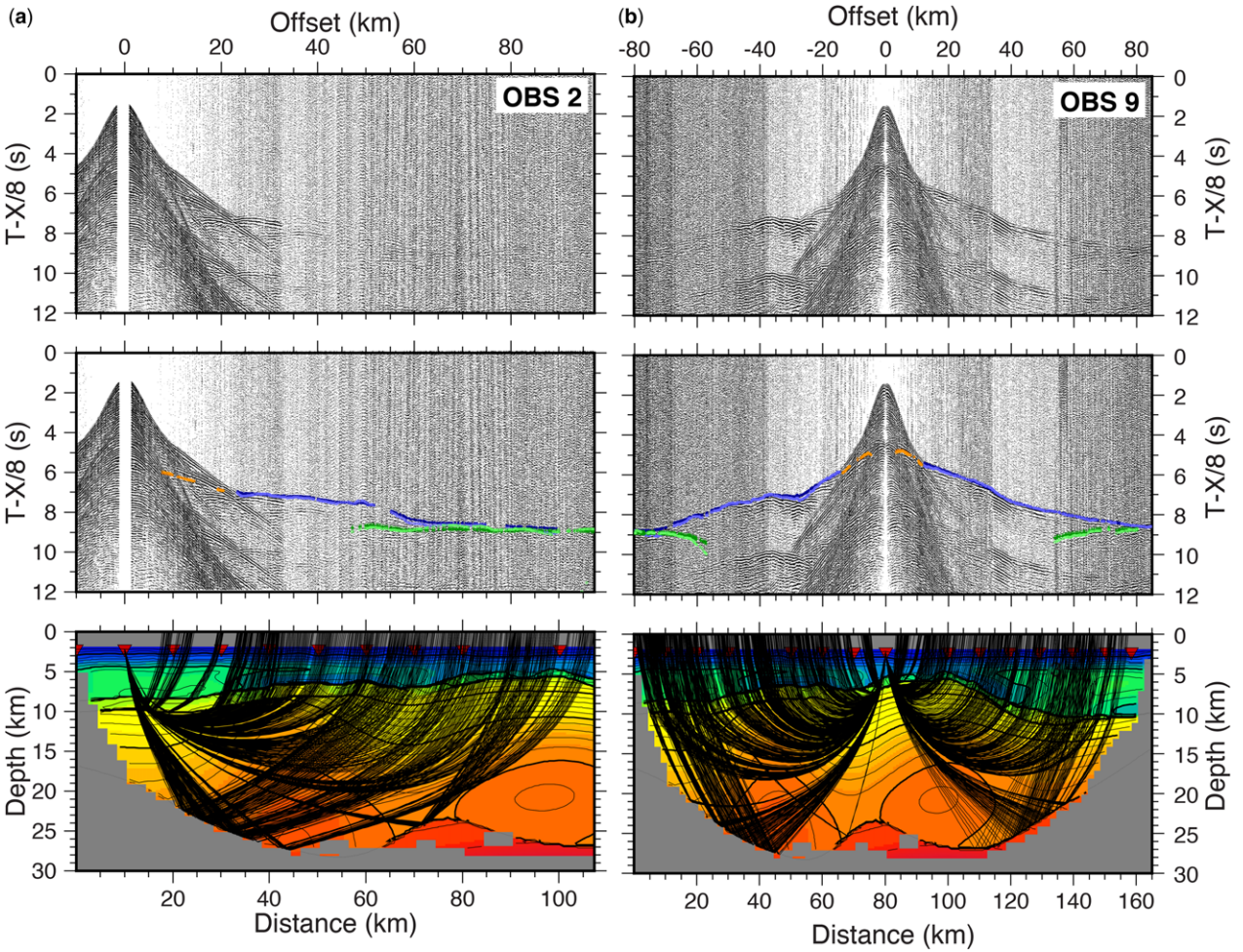

Fig. 3. Receiver gather without picks (top panel). Data with observed picks and picking errors (closed circles and bars) and predicted picks (solid, lighter coloured circles) (middle panel). Orange, PprP; blue, Pg; green, PmP; red, Pn. Ray paths through the final model from the reflection/refraction tomography model (lower panel). (**a**) OBS 2 and (**b**) OBS9.

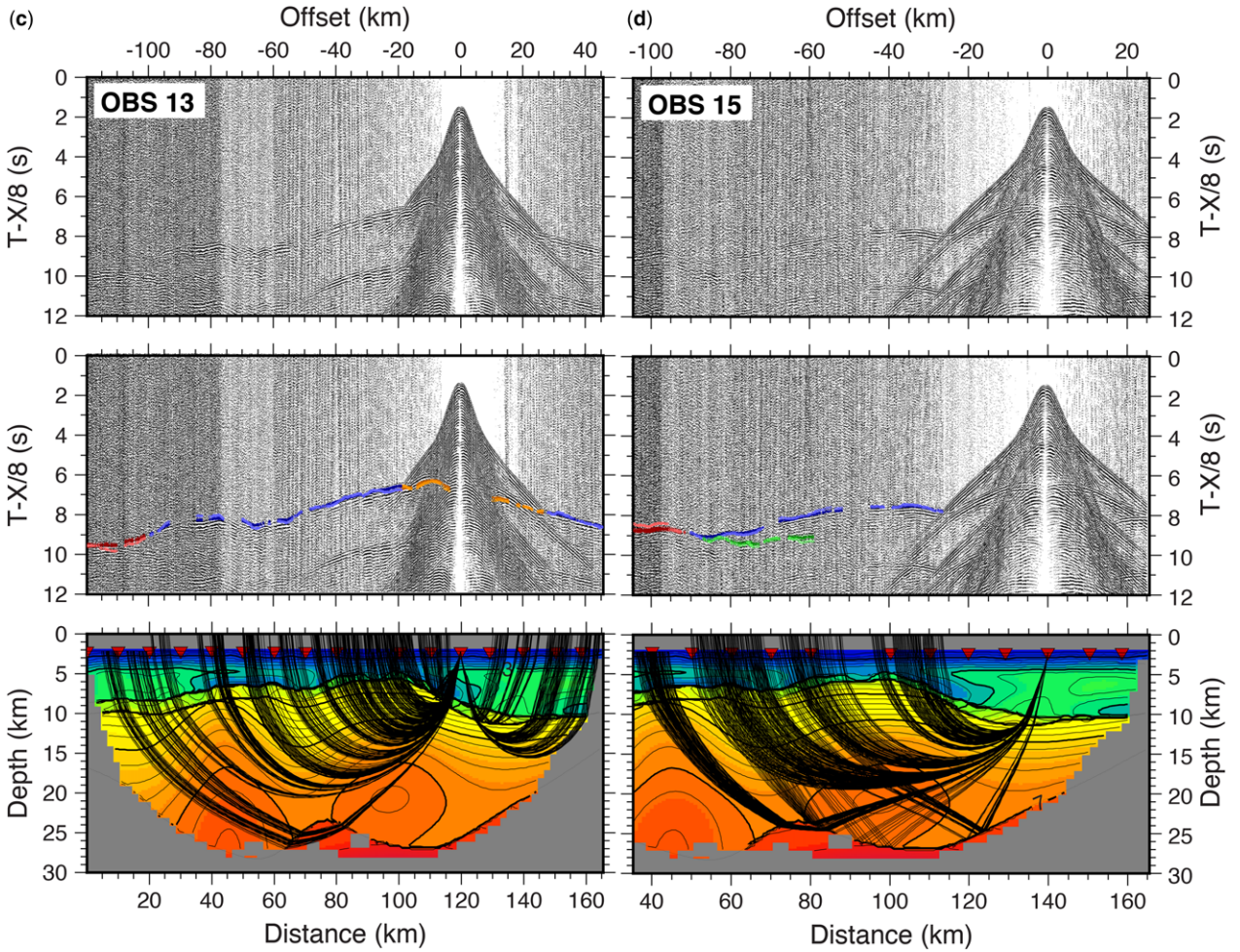

Fig. 3. (**c**) OBS13 and (**d**) OBS15.

Table 2. *Misfits by phase*

Phase	Number picks	Chi squared	RMS misfit (s)
PprP	866	3.442881645	0.129567735
Pg	5334	2.038537344	0.106868266
PmP	1502	2.182268919	0.182210481
Pn	249	2.604642144	0.200007259

chi-squared misfit is 1.65, and the RMS residual is 90 ms.

The first-arrival inversion for the crust and upper mantle structure used 5732 picks. The final model has a chi-squared value of 0.96 and an RMS residual of 76 ms. The reflection/refraction inversion used 7085 picks. The final model has a chi-squared value of 2.23 and an RMS residual of 127 ms.

Based on ray coverage, data fit and testing of different inversion parameterizations, we discuss the confidence that should be placed in different features of our final models. The upper-crustal structure is very well sampled by ray coverage associated with our travel-time picks, and refractions from this part of the model have relatively low misfits (Figs 3–5). Similar features are apparent in both the reflection/refraction tomography and the first-arrival tomography. Thus, we consider the variations in upper-crustal velocity structure between the Andrusov and Archangelsky ridges to be a robust result (Figs 4b & 5b). The lowermost crustal sections beneath the Andrusov and Archangelsky ridges are only constrained by sparse turning wave coverage and relatively sparse reflections from the base of the crust (Figs 3 & 5). Because the uppermost part of the lower crust is sampled by reversed refracted arrivals, we are confident that high velocities are required. However, we cannot constrain the velocity gradient of the lowermost crust or absolute velocity at the very base of the lower crust, and there are thus trade-offs between velocities in the lowermost crust and depth to the base of the crust. Both wide-angle reflections and vertically incident reflections constrain the interpreted pre-rift sedimentary layer on top of the MBSH. We find relatively high data misfits for phases defining this layer (Table 2), which we attribute to substantial lateral variability that cannot be accounted for in the analysis of OBS spaced at approximately 15 km. However, we think that the large-scale patterns of thickness and velocity are well constrained.

Although we obtained an excellent misfit for the first-arrival tomography model (chi-squared value of 0.96), our favoured model from reflection/refraction tomography has a higher chi-squared value of 2.23. We relaxed the data misfit criteria to obtain a relatively smooth model; models with better data fit were substantially rougher. We feel this choice is justified by the likely three-dimensionality of velocity structure beneath these complex ridges, and the complexity of sedimentary, crustal and upper-mantle phases observed on OBS.

Results and discussion

The final velocity models across the Mid Black Sea High provide constraints on the deep sedimentary and crustal structure of this composite ridge.

Sedimentary rocks overlying the Mid Black Sea High

The flat-lying post-rift sedimentary rocks exhibit a low-velocity zone in the Miocene Maikop Formation (Figs 5 & 6) that extends across the eastern basin, and also appears to be present above parts of the MBSH and in the Sinop Trough (Fig. 6) (Scott *et al.* 2009). The low-velocity zone is attributed to fluid overpressure, and fluid pressures close to lithostatic have been inferred (Scott *et al.* 2009), although the application of a more sophisticated approach in the eastern basin (Marin-Moreno *et al.* 2013*a*, *b*) suggests that fluid pressures are lower than those derived from the empirical approaches of Scott *et al.* (2009).

Wide-angle reflections in the OBS data (Fig. 3) and reflections in the reflection profile (Fig. 6) define a distinct layer with a thickness of 1–2 km and velocities of 3.0–4.75 km s^{-1} on top of the Andrusov and Archangelsky ridges (Fig. 5). Based on the character of this layer in the reflection profile, dredging on the Archangelsky Ridge and drilling of the Andrusov Ridge, we interpret this layer to represent a sequence of pre-rift Upper Cretaceous sedimentary rocks (Rudat *et al.* 1993; Aydemir & Demirer 2013). This layer is characterized by brightly reflective layering in the reflection profile, which is consistent with a sedimentary origin (Figs 2 & 6). Drilling on Andrusov Ridge at Sinop-1 recovered a relatively thin layer of Upper Cretaceous carbonate rocks (Aydemir & Demirer 2013). Aydemir & Demirer (2013) suggested that the thickness of this interval would be strongly controlled by basement topography at the time of deposition and thus be highly variable, which may explain why we appear to observe a thicker Upper Cretaceous layer on Profile 4. A similar sequence overlies the Shatsky Ridge to the north (Fig. 1) (Robinson *et al.* 1996; Nikishin *et al.* 2015*a*).

The base of this layer is marked by a bright, continuous reflection in the reflection profile (Fig. 6), which has been interpreted to mark the top of Lower Cretaceous platform carbonate rocks (Rudat *et al.* 1993; Robinson *et al.* 1996). Based on dredging

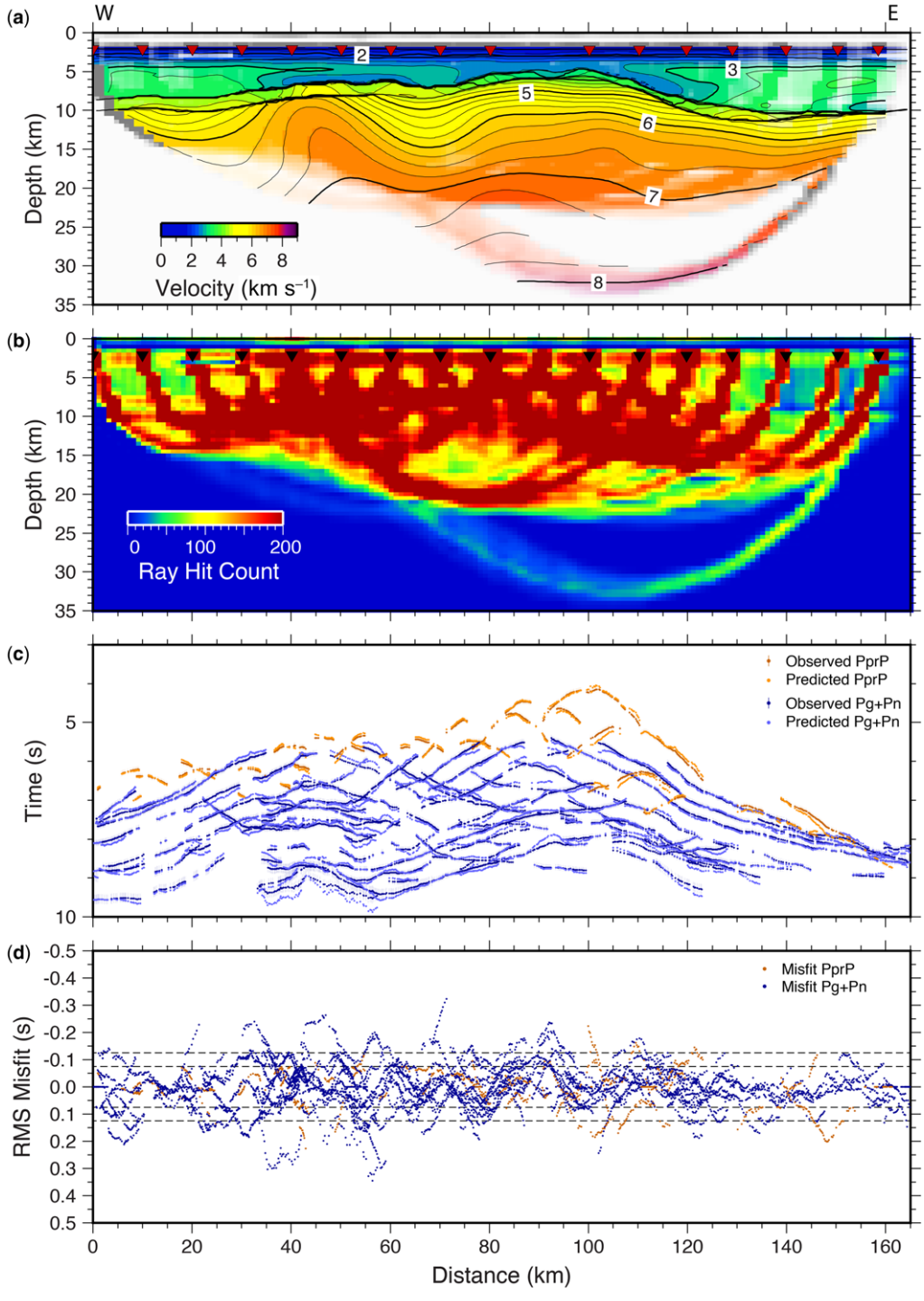

Fig. 4. (**a**) Result of inversion for pre-rift sedimentary reflections (PprP) and first-arriving refractions from crust and upper mantle (Pg and Pn). Velocities contoured at 0.25 km s^{-1}. The velocity model is masked by the density of ray coverage. (**b**) Density of ray coverage over the velocity model in (a). (**c**) Observed and predicted travel-time picks. The uncertainty of observed picks is indicated with bars. (**d**) Travel-time residuals for picks.

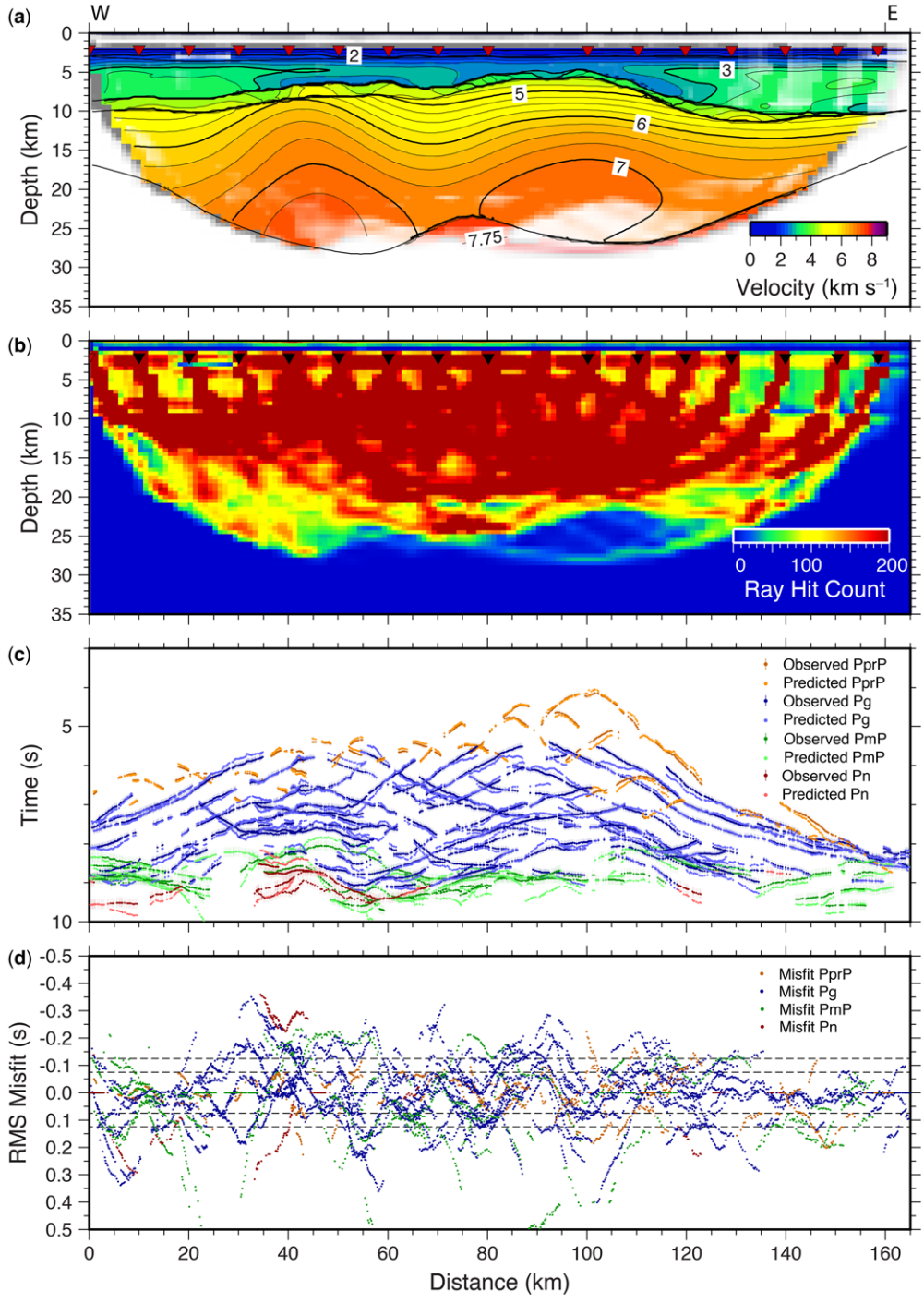

Fig. 5. (**a**) Result of inversion for pre-rift sedimentary reflections (PprP), first-arriving refractions from crust and upper mantle (Pg and Pn), and reflections from the base of the crust (PmP). Velocities are contoured at 0.25 km s^{-1}. The velocity model is masked by the density of ray coverage. (**b**) Density of ray coverage over the velocity model in (a). (**c**) Observed and predicted travel-time picks. The uncertainty of observed picks is indicated with bars. (**d**) Travel-time residuals for picks.

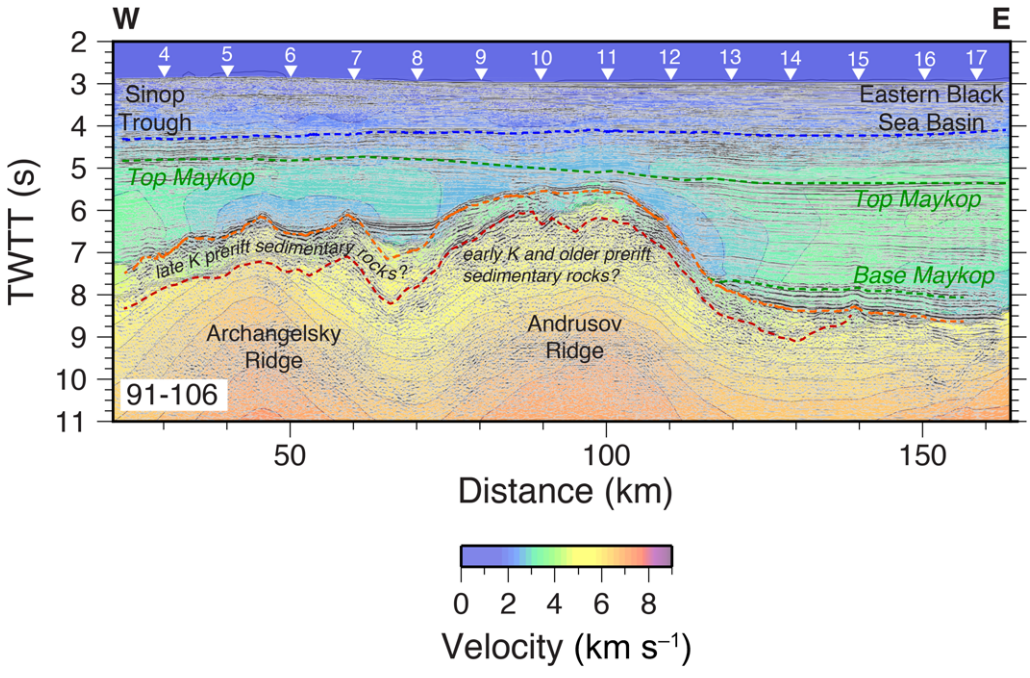

Fig. 6. Overlay of reflection profile 91–106 on the final velocity model from reflection/refraction tomography (Fig. 5), which was converted to two-way travel time.

results on the shallow part of the Archangelsky Ridge, we interpret the uppermost basement beneath this reflection as being composed of Lower Cretaceous platform carbonate rocks and other older pre-rift sedimentary rocks. Platform carbonate rocks are expected to have similar P-wave velocities to upper crystalline crust (Christensen & Mooney 1995), so it is not possible for us to definitively identify carbonate rocks or quantify their thickness, but the nearby dredging results suggest that pre-rift sedimentary rocks are likely to be present in the uppermost basement here. The uppermost basement beneath the prominent reflection described above reaches 6–6.25 km s^{-1} beneath the top of the Archangelsky Ridge, and drops to approximately 4.5 km s^{-1} beneath the Andrusov Ridge. The overlying layer interpreted to represent Upper Cretaceous pre-rift sedimentary rocks also has significantly higher velocities beneath Archangelsky Ridge than beneath Andrusov Ridge. These differences may be attributed to several factors. First, although Archangelsky Ridge is generally a shallower feature (Fig. 1), at the location of Profile 4 it is more deeply buried, so the pre-rift sedimentary rocks may have undergone greater compaction and diagenesis. Secondly, seismic reflection data suggest that the Andrusov Ridge is disrupted by more faults than the Archangelsky Ridge (Robinson *et al.* 1996), and fracturing associated with these faults may reduce the velocity by creating zones of higher porosity and/or causing an elongation of pores, which have a bigger impact on elastic properties (Töksöz *et al.* 1976). Thirdly, other differences in lithology may contribute to observed variations in velocity. Finally, the low-velocity layer in the post-rift directly abuts the Andrusov Ridge, but is separated from Archangelsky Ridge by a layer of higher-velocity material. Therefore, it is possible that fluid overpressure is transmitted into pre-rift sedimentary rocks on the Andrusov Ridge but not on the Archangelsky Ridge.

Crustal structure and implications for tectonic evolution

The Andrusov and Archangelsky ridges exhibit distinctly different crustal velocity structures. As described in the previous subsection, the Archangelsky Ridge has higher velocities in the uppermost basement (6–6.25 km s^{-1}) and a relatively low velocity gradient (*c.* 0.075 km s^{-1} km^{-1}). In contrast, the Andrusov Ridge has velocities in the shallow basement as low as 4.5 km s^{-1} and a high velocity gradient in the upper 10 km of 0.25 km s^{-1} km^{-1}. These differences might be associated with different degrees of fracturing of platform carbonate rocks

(see the previous subsection) or of crystalline rocks, or might arise because the pre-rift sedimentary sequence within the basement is thicker beneath Andrusov Ridge, as perhaps suggested by seismic reflection data (Fig. 2).

Beneath both ridges, the velocity gradient is smaller in the lower crust, and velocities reach a maximum of 7.2–7.3 km s^{-1} at the base of the crust (Fig. 5). These velocities are somewhat higher than those observed beneath Archangelsky Ridge on Profile 3 (*c.* 6.75–7 km s^{-1}) (Shillington *et al.* 2009) (Fig. 1), and may indicate the presence of a more mafic pre-rift crust (e.g. Christensen & Mooney 1995). Rifting to form the eastern Black Sea occurred in a series of terranes accreted to the Euroasian margin, which include volcanic arcs and oceanic plateaux, both of which are typified by high-velocity lower crust in modern analogues (Shillington *et al.* 2004; Kodaira *et al.* 2007; Calvert 2011).

These velocities are also only slightly lower than lower-crustal velocities observed in crust within the centre of the eastern part of the eastern Basin (Shillington *et al.* 2009), which were interpreted as evidence for new magmatic crust formed during magma-rich rifting and early spreading. However, the relationship between lower-crustal velocity and crustal thickness suggests that syn-rift magmatism is not responsible for the high lower-crustal velocities beneath the MBSH. In the eastern part of the Eastern Basin (Shillington *et al.* 2009) and at other volcanic rifted margins worldwide (e.g. Holbrook & Kelemen 1993; White *et al.* 2008), high-velocity lower crust (*c.* 7.4–7.5 km s^{-1}) interpreted to represent mafic synrift intrusions is most prominent in the area of crustal thinning. In contrast, the highest velocities observed beneath the MBSH occur in the thickest crust and do not increase towards the thinned margins of the ridge. Consequently, we propose that high lower-crustal velocities beneath the MBSH represent high velocities associated with accreted volcanic arcs and oceanic plateaux in the pre-rift crust. Hence, our observations from Profile 4 is consistent with the view that extension in the western part of the Eastern Black Sea Basin was largely amagmatic (Shillington *et al.* 2009).

The crustal layer, which may include platform carbonate rocks and possibly other pre-rift sedimentary rocks, thickens beneath both ridges to reach a maximum of 20–23 km (Fig. 5). Between the two ridges, it decreases to approximately 16 km, providing evidence that the modest increase in sediment thickness between the two ridges (Fig. 1) is associated with crustal-scale extension. Although the Archangelsky Ridge is deeply buried at the location of Profile 4 (Fig. 1), it clearly remains a major crustal feature at this location. Uppermost mantle velocities are a little below 8 km s^{-1}. Based on teleseismic receiver functions, gravity data and limited wide-angle seismic constraints, the crustal thickness onshore Turkey in the vicinity of Archangelsky Ridge is approximately 35 km (Özacar *et al.* 2010; Yegorova *et al.* 2013), with thicker crust farther east where it is affected more by compressional deformation. Therefore, the crust along Profile 4 has been thinned by a factor of 1.5–2. The degree of thinning is somewhat lower than inferred by Shillington *et al.* (2008) based on the relationship between sediment thickness and thinning factor on a well-constrained profile; this relationship gives a thinning factor of 2–2.5 along most of Profile 4 (Fig. 7). One possible explanation for this difference is that the 'crust' of the MBSH may include sections of pre-rift sedimentary rocks that are not a part of the unthinned crustal section onshore (Okay *et al.* 2017).

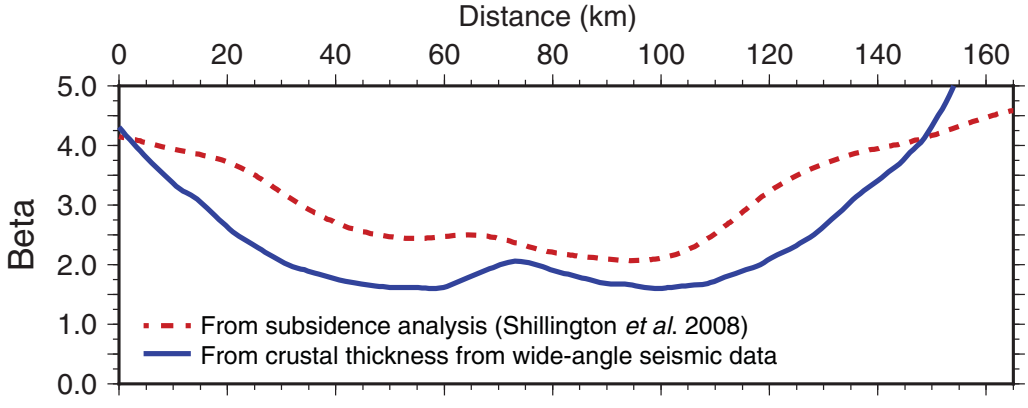

Fig. 7. Comparison of the crustal thinning factor (beta = initial thickness/rifted thickness) along Line 4 from subsidence analysis based on sediment thickness (Shillington *et al.* 2008) and from this study assuming an initial crustal thickness of 35 km.

Conclusions

From our analysis of data from a wide-angle seismic profile across the Mid Black Sea High, comprising the en echelon Archangelsky and Andrusov ridges, we conclude that:

- The basement highs are covered by at least a 1- to 2-km-thick layer of pre-rift sedimentary rocks overlying a higher-velocity basement that may include pre-rift sedimentary rocks, including platform carbonates that cannot be readily distinguished from the underlying crystalline crust.
- The pre-rift sedimentary rocks and upper basement have higher velocities on the Archangelsky Ridge and lower velocities on the Andrusov Ridge. These differences could be explained by different amounts of faulting or changes in the abundance and/or composition of pre-rift sedimentary rocks.
- The lower crust has a low velocity gradient, and velocities exceed 7.0 km s^{-1} at its base; the velocity structure is consistent with the presence of a mafic pre-rift crust with little magmatic addition during rifting.
- The crust is 20–23 km thick beneath the ridges and approximately 16 km thick between them, representing thinning factors of 1.5–2.0 compared to adjacent crust in NE Turkey.

We thank T. Besevli, G. Coskun, A. Demirer, M. Erduran, S. Jones, R. O'Connor, B. Peterson, A. Price, K. Raven and M. Shaw-Champion, and the officers, crew and technical team aboard R/V *Iskatel* for their support during the acquisition and analysis of this dataset. This work was supported by the Natural Environment Research Council (UK) (NER/T/S/2003/00114 and NER/T/S/2003/00885), BP and the Turkish Petroleum Company (TPAO). BP and TPAO generously provided access to the seismic reflection data. We also thank N. Hodgson and an anonymous reviewer for constructive comments that greatly improved the manuscript.

References

AYDEMIR,V. & DEMIRER, A. 2013. Upper Cretaceous and Paleocene shallow water carbonates along the Pontide Belt. *In*: *19th International Petroleum and Natural Gas Congress and Exhibition of Turkey, 15–17 May 2013*, Turkish Association of Petroleum Geologists, Ankara, 284–290.

BANKS, C.J., ROBINSON, A.G. & WILLIAMS, M.P. 1997. *Structure and Regional Tectonics of the Achara-Trialet Fold Belt and the Adjacent Rioni and Kartli Foreland Basins*. American Association of Petroleum Geologists, Tulsa, OK.

BELOUSOV, V.V., VOLVOVSKY, B.S. *ET AL.* 1988. Structure and evolution of the earth's crust and upper mantle of the Black Sea. *Bollettino Di Geofisica Teorica ed Applicata*, **30**, 109–196.

CALVERT, A.J. 2011. The seismic structure of island arc crust. *In*: BROWN, D. & RYAN, P.D. (eds) *Arc–Continent Collision*. Springer, Berlin, 87–119.

CHRISTENSEN, N.I. & MOONEY, W.D. 1995. Seismic velocity structure and composition of the continental crust – a global view. *Journal of Geophysical Research: Solid Earth*, **100**, 9761–9788.

ESPURT, N., HIPPOLYTE, J.C., KAYMAKCI, N. & SANGU, E. 2014. Lithospheric structural control on inversion of the southern margin of the Black Sea Basin, Central Pontides, Turkey. *Lithosphere*, **6**, 26–34.

GOBARENKO, V.S., MUROVSKAYA, A.V., YEGOROVA, T.P. & SHEREMET, E.E. 2016. Collision processes at the northern margin of the Black Sea. *Geotectonics*, **50**, 407–424.

GÖRÜR, N. 1988. Timing of opening of the Black Sea basin. *Tectonophysics*, **147**, 247–262.

HOBRO, J.W.D., SINGH, S.C. & MINSHULL, T.A. 2003. Three-dimensional tomographic inversion of combined reflection and refraction seismic traveltime data. *Geophysical Journal International* **152**, 79–93.

HOLBROOK, W.S. & KELEMEN, P.B. 1993. Large igneous province on the US Atlantic margin and implications for magmatism during continental breakup. *Nature*, **364**, 433–436.

KAZMIN, V.G., SCHREIDER, A.A. & BULYCHEV, A.A. 2000. Early stages of evolution of the Black Sea. *In*: BOZKURT, E., WINCHESTER, J.A. & PIPER, J.D.A. (eds) *Tectonics and Magmatism in Turkey and the Surrounding Area*. Geological Society, London, Special Publications, **173**, 235–249, https://doi.org/10.1144/GSL.SP.2000.173.01.12

KODAIRA, S., SATO, T., TAKAHASHI, N., ITO, A., TAMURA, Y., TATSUMI, Y. & KANEDA, Y. 2007. Seismological evidence for variable growth of crust along the Izu intra-oceanic arc. *Journal of Geophysical Research*, **112**, B05104.

LETOUZEY, J., BIJU-DUVAL, B., DORKEL, A., GONNARD, R., KRISTCHEV, K., MONTADERT, L. & SUNGURLU, O. 1977. The Black Sea: A marginal basin, geophysical and geological data. *In*: BIJU-DUVAL, B. & MONTADERT, L. (eds) *International Symposium of the Mediterranean Basins*. Editions Technip, Paris, 363–376.

MARIN-MORENO, H., MINSHULL, T.A. & EDWARDS, R.A. 2013*a*. Inverse modelling and seismic data constraints on overpressure generation by disequilibrium compaction and aquathermal pressuring: application to the Eastern Black Sea Basin. *Geophysical Journal International*, **194**, 814–833.

MARIN-MORENO, H., MINSHULL, T.A. & EDWARDS, R.A. 2013*b*. A disequilibrium compaction model constrained by seismic data and application to overpressure generation in the Eastern Black Sea Basin. *Basin Research*, **25**, 331–347.

MINSHULL, T.A., WHITE, N.J. *ET AL.* 2005. Seismic data reveal eastern Black Sea structure. *Eos*, **86**, 416–417.

NIKISHIN, A.M., KOROTAEV, M.V., ERSHOV, A.V. & BRUNET, M.-F. 2003. The Black Sea basin: tectonic history and Neogene–Quaternary rapid subsidence modelling. *Sedimentary Geology*, **156**, 149–168.

NIKISHIN, A.M., OKAY, A.I., TUYSUZ, O., DEMIRER, A., AMELIN, N. & PETROV, E. 2015*a*. The Black Sea basins structure and history: new model based on new deep penetration regional seismic data. Part 1: basins

structure and fill. *Marine and Petroleum Geology*, **59**, 638–655.

Nikishin, A.M., Okay, A., Tuysuz, O., Demirer, A., Wannier, M., Amelin, N. & Petrov, E. 2015*b*. The Black Sea basins structure and history: new model based on new deep penetration regional seismic data. Part 2: tectonic history and paleogeography. *Marine and Petroleum Geology*, **59**, 656–670.

Okay, A.I., Sengor, A.M.C. & Görür, N. 1994. Kinematic history of the opening of the Black Sea and its effect on the surrounding regions. *Geology*, **22**, 267–270.

Okay, A.I., Sunal, G., Sherlock, S., Altiner, D., Tüysüz, O., Kylander-Clark, A.R.C. & Aygül, M. 2013. Early Cretaceous sedimentation and orogeny on the active margin of Eurasia: Southern Central Pontides, Turkey. *Tectonics*, **32**, 1247–1271.

Okay, A.I., Altiner, D., Sunal, G., Aygül, M., Akdoğan, R., Altiner, S. & Simmons, M. 2017. Geological evolution of the Central Pontides. *In*: Simmons, M.D., Tari, G.C. & Okay, A.I. (eds) *Petroleum Geology of the Black Sea*. Geological Society, London, Special Publications, **464**, https://doi.org/10.1144/SP464.3

Özacar, A.A., Zandt, G., Gilbert, H. & Beck, S.L. 2010. Seismic images of crustal variations beneath the East Anatolian Plateau (Turkey) from teleseismic receiver functions. *In*: Sosson, M., Kaymakci, N., Stephenson, R.A., Bergerat, F. & Starostenko, V. (eds) *Sedimentary Basin Tectonics from the Black Sea and Caucasus to the Arabian Platform*. Geological Society, London, Special Publications, **340**, 485–496, https://doi.org/10.1144/SP340.21

Rangin, C., Bader, A.G., Pascal, G., Ecevitoglu, B. & Görür, N. 2002. Deep structure of the Mid Black Sea High (offshore Turkey) imaged by multi-channel seismic survey (BLACKSIS cruise). *Marine Geology*, **182**, 265–278.

Robertson, A.H.F., Ustaömer, T., Pickett, E.A., Collins, A.S., Andrew, T. & Dixon, J.E. 2004. Testing models of Late Palaeozoic–Early Mesozoic orogeny in Western Turkey: support for an evolving open-Tethys model. *Journal of the Geological Society, London*, **161**, 501–511, https://doi.org/10.1144/0016-764903-080

Robinson, A.G., Banks, C.J., Rutherford, M.M. & Hirst, J.P.P. 1995. Stratigraphic and structural development of the Eastern Pontides, Turkey. *Journal of the Geological Society, London*, **152**, 861–872, https://doi.org/10.1144/gsjgs.152.5.0861

Robinson, A.G., Rudat, J.H., Banks, C.J. & Wiles, R.L.F. 1996. Petroleum geology of the Black Sea. *Marine and Petroleum Geology*, **13**, 195–223.

Rudat, J.H., MacGregor, D.S. & Ignatov, A.M. 1993. Unconventional exploration techniques in a high cost deepwater basin: a case study from the Black Sea. *SEG Technical Program Expanded Abstracts*, **1993**, 1351.

Saintot, A. & Angelier, J. 2002. Tectonic paleostress fields and structural evolution of the NW-Caucaus fold-and-thrust belt from Late Cretaceous to Quaternary. *Tectonophysics*, **357**, 1–31.

Scott, C.L., Shillington, D.J., Minshull, T.A., Edwards, R.A., Brown, P.J. & White, N.J. 2009. Wide-angle seismic data reveal extensive overpressures in Eastern Black Sea. *Geophysical Journal International*, **178**, 1145–1163, https://doi.org/10.1111/j.1365-246X.2009.04215.x

Shillington, D.J., Van Avendonk, H.J.A., Holbrook, W.S., Kelemen, P.B. & Hornbach, M.J. 2004. Composition and structure of the central Aleutian island arc from arc-parallel wide-angle seismic data. *Geochemistry, Geophysics, Geosystems*, **5**, Q10006, https://doi.org/10.1029/2004GC000715

Shillington, D.J., White, N., Minshull, T.A., Edwards, G.R.H., Jones, S., Edwards, R.A. & Scott, C.L. 2008. Cenozoic evolution of the eastern Black Sea: a test of depth-dependent stretching models. *Earth and Planetary Science Letters*, **265**, 360–378.

Shillington, D.J., Scott, C.L., Minshull, T.A., Edwards, R.A., Brown, P.J. & White, N. 2009. Abrupt transition from magma-starved to magma-rich rifting in the eastern Black Sea. *Geology*, **37**, 7–10, https://doi.org/10.1130/G25302A.1

Starostenko, V., Buryanov, V. *et al.* 2004. Topography of the crust-mantle boundary beneath the Black Sea Basin. *Tectonophysics*, **381**, 211–233.

Tari,G., Schleder, Zs., Fallah, M., Turi, V., Kosi, W. & Krezsek, Cs. 2015. Regional rift structure of the Western Black Sea Basin: map-view kinematics. *In*: *Transactions of the GCSSEPM Foundation Perkins-Rosen 34th Annual Research Conference 'Petroleum Systems in Rift Basins'*, Houston, Texas, 372–396.

Töksöz, M.N., Cheng, C.H. & Timur, A. 1976. Velocities of seismic waves in porous rocks. *Geophysics*, **41**, 621–645.

Vincent, S.J., Allen, M.B., Ismail-Zadeh, A.D., Flecker, R., Foland, K.A. & Simmons, M.D. 2005. Insights from the Talysh of Azerbaijan into the Paleogene evolution of the South Caspian region. *GSA Bulletin*, **117**, 1513–1533.

White, R.S., Smith, L.K., Roberts, A.W., Christie, P.A.F., Kusznir, N.J. & iSIMM Team 2008. Lower-crustal intrusion on the North Atlantic continental margin. *Nature*, **452**, 460–465.

Yegorova, T. & Gobarenko, V. 2010. Structure of the Earth's crust and upper mantle of the West- and East-Black Sea Basins revealed from geophysical data and its tectonic implications. *In*: Sosson, M., Kaymakci, N., Stephenson, R.A., Bergerat, F. & Starostenko, V. (eds) *Sedimentary Basin Tectonics from the Black Sea and Caucasus to the Arabian Platform*. Geological Society, London, Special Publications, **340**, 23–42, https://doi.org/10.1144/SP340.3

Yegorova, T., Gobarenko, V. & Yanovskaya, T. 2013. Lithosphere structure of the Black Sea from 3-D gravity analysis and seismic tomography. *Geophysical Journal International*, **193**, 287–303.

Yilmaz, Y., Tüysüz, O., Yigitbas, E., Can Genç, S. & Sengör, A.M.C. 1997. Geology and tectonic evolution of the Pontides. *In*: Robinson, A.G. (ed.) *Regional and Petroleum Geology of the Black Sea and Surrounding Region*. American Association of Petroleum Geologists Memoirs, **68**, 183–226.

Zonenshain, L.P. & Le Pichon, X. 1986. Deep basins of the Black Sea and Caspian Sea as remnants of Mesozoic back-arc basins. *Tectonophysics*, **123**, 181–211.